CellPress

Developmental Cell

Review

Mechanics of Development

Katharine Goodwin[1] and Celeste M. Nelson[2,3,*]
[1]Lewis-Sigler Institute for Integrative Genomics, Princeton University, Princeton, NJ 08544, USA
[2]Department of Chemical and Biological Engineering, Princeton University, Princeton, NJ 08544, USA
[3]Department of Molecular Biology, Princeton University, Princeton, NJ 08544, USA
*Correspondence: celesten@princeton.edu
https://doi.org/10.1016/j.devcel.2020.11.025

SUMMARY

Mechanical forces are integral to development—from the earliest stages of embryogenesis to the construction and differentiation of complex organs. Advances in imaging and biophysical tools have allowed us to delve into the developmental mechanobiology of increasingly complex organs and organisms. Here, we focus on recent work that highlights the diversity and importance of mechanical influences during morphogenesis. Developing tissues experience intrinsic mechanical signals from active forces and changes to tissue mechanical properties as well as extrinsic mechanical signals, including constraint and compression, pressure, and shear forces. Finally, we suggest promising avenues for future work in this rapidly expanding field.

INTRODUCTION

Much of developmental biology has sought to uncover the roles of morphogens and the molecular programs that drive development (Briscoe and Small, 2015; Freeman and Gurdon, 2002; Kicheva and Briscoe, 2015). More recently, attention has turned to studying how mechanical forces influence developing tissues and understanding the physical mechanisms of morphogenesis (Anlaş and Nelson, 2018; Mammoto and Ingber, 2010; Stooke-Vaughan and Campàs, 2018). These two schools of thought are not necessarily separate; indeed, local mechanical properties and their effects on tissue topology can shape morphogen fields (Manning et al., 2015; Shyer et al., 2015), and cell displacements can change how a tissue experiences a static molecular gradient (Nerurkar et al., 2019).

Mechanical forces influence all stages of development, from the early embryo, to gastrulation and establishment of the body plan, to organogenesis. Pioneering reviews laid the foundation for our current appreciation of the role of mechanical forces in development (Beloussov et al., 1994; Keller et al., 2003; Wolpert, 1971), and over the past 10 years, advances in animal models, live-imaging approaches, and biophysical measurements have shed light on the mechanics of morphogenesis (Ayad et al., 2019). In particular, these advances have allowed us to extend principles of developmental mechanobiology that were first established primarily in invertebrate embryos (Heisenberg and Bellaïche, 2013; Lecuit and Lenne, 2007; Mammoto and Ingber, 2010) to the morphogenesis of larger, more complex, and less accessible organs and organisms.

Here, we provide an overview of different kinds of mechanical forces that drive morphogenesis and highlight recent progress in understanding how they regulate developmental processes—from the earliest stages of embryogenesis to the finishing touches of organogenesis. We include examples of intrinsic mechanics driving morphogenesis, including the generation of active forces and tuning of tissue fluidity, as well as examples of extrinsic mechanical signals, such as physical constraints and microenvironment mechanics, static and dynamic pressures, and shear forces from fluid flow. In this review, we focus on how mechanical forces directly influence tissue form. However, it is important to note that mechanical forces also influence another key aspect of development—cellular differentiation, in which physical forces activate intracellular signaling cascades or change nuclear envelope mechanics to regulate the activation or nuclear localization of mechanosensitive transcription factors, leading to downstream changes in gene expression and altering cell behavior and fate (Hampoelz and Lecuit, 2011; Kumar et al., 2017; Vining and Mooney, 2017). These changes at the nuclear level could indirectly influence the material properties of the tissue and thus changes in tissue form.

Tension and Active Forces

Actomyosin networks coupled to cell-cell and cell-extracellular matrix (ECM) adhesions are responsible for generating the forces required for cells to pull on their neighbors or on their underlying substratum (Hoffman et al., 2011). Actomyosin contractions can locally constrict parts of the cell, as in apical constriction, in order to change cell shape or allow it to exert traction in order to move over a surface, as in cell migration. These active forces at the level of single cells can be translated into dramatic changes in shape at the tissue level. Actomyosin networks often contract with pulsatile dynamics. Indeed, pulsed actomyosin contractions are an evolutionarily conserved mechanism for driving tissue morphogenesis. These contractions promote ventral-furrow ingression in *Drosophila* (Martin et al., 2009), compaction in the mouse blastocyst (Maître et al., 2015), and have even been observed in collectives of unicellular organisms which form sheets that can fold in response to light (Brunet et al., 2019).

Active forces generated by actomyosin networks orchestrate cell-shape changes required for transforming the early mouse

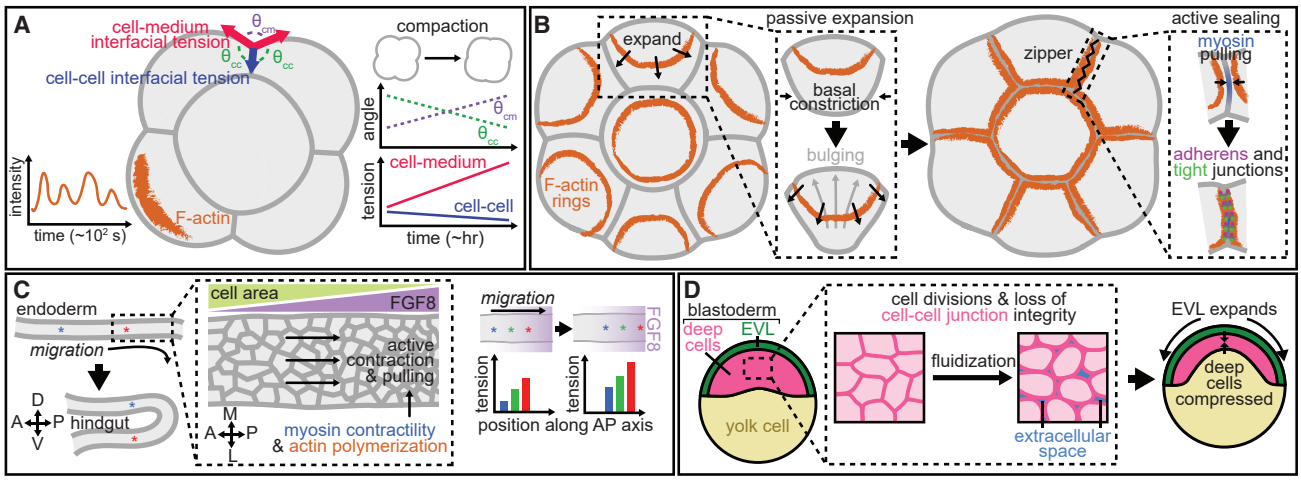

Figure 1. Intrinsic Mechanical Forces Driving Morphogenesis

(A) During compaction of the 8-cell embryo, tension at the cell-medium interface increases, changing the angles between cells. The increase in tension is accompanied by pulsatile actin dynamics at the cell cortex.

(B) Apical actin rings in the 16-cell mouse embryo expand toward intercellular junctions to seal the blastocyst.

(C) Hindgut morphogenesis in the chick embryo requires the gut endoderm to fold over onto itself to form the gut tube. This movement is generated by collective cell migration resulting from a gradient of cell contractility that interacts with a stable morphogen gradient to drive tissue flow.

(D) Deep cells fluidize at the onset of zebrafish epiboly as they undergo divisions and lose integrity of their cell-cell contacts. As a result, the expanding EVL compresses the deep-cell layer to drive blastoderm thinning.

embryo from an agglomeration of roughly spherical cells into a compacted embryo and then into a hollow blastocyst. As the embryo compacts, the angle between adjacent cells at the periphery of the embryo increases and the surface tension at the cell-medium interface increases (Figure 1A; Table 1) (Maître et al., 2015). Consistently, actomyosin activity is enriched at the cell-medium interface compared with cell-cell interfaces, and the increase in tension at the cell-medium interface requires actin polymerization and myosin activity. Strikingly, this increase in tension is cell autonomous (occurs even in dissociated cells) and is accompanied by oscillatory cell deformations and actin accumulation; whether the oscillations themselves are required for compaction has yet to be shown. Cells of the 8-cell embryo also extend cadherin-containing filopodia over their neighbors that deform the apical part of the cell to drive compaction (Fierro-González et al., 2013).

From the 8-cell stage to the 16-cell stage, a subset of cells ends up in the center of the embryo. These inner cells give rise to the embryonic tissues and the primitive endoderm, whereas the outer cells (the trophectoderm) give rise to extraembryonic tissues that encapsulate the embryo. Inner cells are positioned by apical constriction (Maître et al., 2016; Samarage et al., 2015). Myosin is enriched at constricting intercellular junctions, and laser ablation revealed more recoil (a proxy for cortical tension) along junctions between constricting cells and their neighbors than between non-constricting cells. Furthermore, ablations oriented perpendicular to junctions between constricting cells caused more recoil of the cortical actin network than ablations parallel to junctions, demonstrating that the apical cortex of constricting cells is under greater tension. Specification and positioning of trophectoderm cells may also be mechanically regulated—keratin-rich intermediate filaments stabilize F-actin within the apical domain and additionally serve as an asymmetrically inherited structural component that predicts trophectoderm fate (Lim et al., 2020).

During the next major phase of mouse embryogenesis (16- to 32-cell stages), the embryo transforms from a solid mass of cells (called the morula) to a fluid-filled blastocyst with an inner cell mass (ICM) and an outer layer of cells called the trophoblast. During this transition, the embryo undergoes additional actomyosin-dependent remodeling in order to seal junctions between the outer cells and to facilitate the formation of a fluid-filled cavity— called the "blastocoel"—within the center of the embryo (Zenker et al., 2018). In the apical (outward-facing) domains of the cells of the 16-cell embryo, actin rings assemble and passively expand until they reach cell-cell junctions (Figure 1B). Actin ring expansion appears to be driven indirectly by constriction of the basal (inward-facing) portion of the cells, which causes the apical portion of the cell to expand and push the actin ring outward. Active processes are then initiated—myosin becomes enriched at the contact between the actin ring and the membrane and helps to capture rings in neighboring cells and pull them to the same contact point. The two actin rings are then zippered together in a myosin- and tension-dependent process that helps to seal the cell-cell junction by recruiting and stabilizing adherens and tight junction components.

Active forces drive the formation of increasingly complex tissue architectures throughout embryogenesis. Actomyosin activity is required for several aspects of neural tube closure, including apical constriction, apical-basal cell lengthening, and cell migration (Nikolopoulou et al., 2017), and for formation of the gut tube (Nerurkar et al., 2019). After gastrulation, the endoderm, which gives rise to the digestive tract and lungs, is transformed from a sheet of cells into a tube. Morphogenesis of the hindgut from the endoderm during embryonic development of the chick involves a gradient in contractile forces that drives coordinated migration of the gut endoderm sheet, allowing it to fold over on itself to generate the gut tube (Nerurkar et al., 2019) (Figure 1C). Cells of the endoderm are exposed to a gradient

Table 1. Physical Concepts and Equations Related to the Mechanics of Development

Physical Concepts	Relevant Quantities	Equations	Examples of Related Biological Processes
Viscoelasticity	Stress (σ) Elastic modulus (E) Viscosity (μ) Displacement (ε) Time (t)	Elastic element $\sigma = E\varepsilon$ Viscous element $\sigma = \mu\frac{ds}{dt}$	Cortical tension and recoil after laser ablation (Samarage et al., 2015; Zenker et al., 2018)
Shape index and the jamming transition	Shape index ($\overline{p}$) Cell area (A) Cell perimeter (P) Critical shape index (p_0)	$\overline{p} = \frac{P}{\sqrt{A}}$ if $\overline{p} > p^0$, the tissue is fluid-like if $\overline{p} < p^0$, the tissue is solid-like	*Drosophila* germband extension (Wang et al., 2020), zebrafish tailbud elongation (Mongera et al., 2018), avian gastrulation (Firmino et al., 2016; Saadaoui et al., 2020)
Differential stiffness driving buckling of a tube attached to a sheet	Buckling wavelength (λ) Elastic modulus of the tube (E_t) Elastic modulus of the sheet (E_s) Moment of inertia of the tube (I_t) Thickness of the sheet (h)	$\lambda \propto \left(\frac{E_t I_t}{E_s h}\right)^{1/3}$	Looping of the avian gut (Savin et al., 2011)
Differential growth driving buckling of a sheet attached to a viscoelastic foundation	Buckling wavelength (λ) Elastic modulus of the sheet (E) Critical in-plane load (N, scales with growth rate)	$\lambda \propto \sqrt{\frac{E}{N}}$	Branching of the mesenchyme-free murine airway epithelium (Varner et al., 2015)
Pressure in a spherical vessel	Stress (σ) Pressure (P) Radius of the vessel (R) Thickness of the walls (t)	$\sigma = \frac{PR}{2t}$	Pressurization of the blastocyst (Chan et al., 2019; Dumortier et al., 2019; Leonavicius et al., 2018), zebrafish inner ear morphogenesis (Hoijman et al., 2015; Mosaliganti et al., 2019)
Young-Laplace equation as applied to micropipette aspiration	Surface tension (γ) Applied pressure (P) Radius of curvature of the aspirated portion of the cell (R_c) Micropipette radius (R_p)	$\gamma = \frac{P}{2\left(\frac{1}{R_p} - \frac{1}{R_c}\right)}$	Surface tension at the cell-medium interface of early mouse embryo (Maître et al., 2015)
Fluid shear stress	Shear stress (τ) Viscosity (μ) Fluid velocity (u) Height above the boundary (y)	$\tau = \mu\frac{du}{dy}$	Zebrafish heart valve morphogenesis (Boselli et al., 2017)

of fibroblast growth factor 8 (FGF8) that is highest at the posterior end of the tissue. Posterior-most cells contract, pulling their trailing neighbors into the region of high FGF8 concentration, causing them to contract as well. This positive feedback generates a gradient of contractile forces that drives tissue elongation.

Actomyosin-driven apical constriction is responsible for generating tissue topology in many different organs. Pulsed actomyosin contractions promote apical constriction during invagination of the *Drosophila* salivary gland (Chung et al., 2017). Surprisingly, apical constrictions are not strictly required for invagination in this context (tissue-wide compressive forces can compensate to induce buckling—a concept discussed below) but are necessary to achieve the correct tissue morphology. In the avian lung, lateral branches form by apical constriction of epithelial cells in the primary bronchus (Kim et al., 2013). This active tissue folding requires growth factor signaling and myosin contractility, but how growth factor signaling elicits localized apical constriction remains unclear. During postnatal development of the murine intestine, crypts form through apical constriction of epithelial cells and "hinge" cells basally constrict to generate a boundary between crypts and villi (Sumigray et al., 2018). The initial step requires myosin activity, whereas the subsequent step depends upon remodeling of cell-cell adhesion; both are necessary to achieve correct tissue architecture and spacing between villi.

Aside from apical constriction, actomyosin-based contractility can drive other cellular behaviors that are important for tissue morphogenesis. For example, contractility drives condensation of dermal progenitors in the avian skin, inducing a mechanosensitive response in the neighboring epidermal cells to initiate specification of feather follicles (Shyer et al., 2017). In the murine hair follicle, actomyosin-mediated rearrangements of epidermal follicle progenitors lead to rotational cell flows that relocate anterior cells to the periphery of the follicle and posterior cells to the center; these rearrangements are required to establish an asymmetric follicle morphology and the constituent cell fates (Cetera et al., 2018). In this case, active forces drive morphogenesis by promoting cell migration and, furthermore, promote patterned differentiation of the murine hair follicle.

Cellular mechanosensing of physical signals such as substratum stiffness and tension can inform fate decisions, even in cells that may not be actively contributing to morphogenetic

movements. For example, airway epithelial cells cultured in tubes of developmentally relevant geometries (wider to mimic proximal airways, narrower to mimic distal airways) experience curvature-dependent tension that is interpreted to dictate the expression of either proximal or distal fate markers (Soleas et al., 2020). Future work will elucidate whether and how the active forces that generate complex tissue topologies are also directly sensed and interpreted by differentiating cells.

Fluid-to-Solid Transitions

Fluidity and solidity have recently emerged as useful descriptors of cell migration that can predict whether cells migrate independently or collectively (or somewhere in between). In fluid-like tissues, cells can rearrange and move past their neighbors, whereas in solid-like tissues, neighbors are maintained and rearrangements are minimal (Bi et al., 2015; Schötz et al., 2013). The transition between these two states is called the ''jamming transition'' and can be predicted in diverse biological systems by changes in cell geometry (Atia et al., 2018; Bi et al., 2015; Wang et al., 2020). This framework has been applied to studies of cancer (Haeger et al., 2014) and asthma (Park et al., 2015) and is increasingly being applied to studies of development.

In simple two-dimensional cell sheets, the jamming transition is predicted to occur when the shape index—a simple parameter that depends on the cell perimeter and area—surpasses a specific value (Table 1). Tissues composed of hexagonal cells have a shape index below this threshold and exhibit solid-like behavior, whereas those with irregularly shaped or elongated cells have a shape index above the threshold and exhibit fluid-like behavior (Bi et al., 2015). However, recent work in *Drosophila* germband extension has shown that the parameters regulating jamming may depend on whether the tissue is experiencing isotropic or anisotropic forces (Wang et al., 2020). Convergent extension is an anisotropic process, and cell shape is insufficient to predict the jamming transition that marks the onset of tissue flow in the germband. An additional parameter describing cell-shape alignment is required to predict these changes and altered cell behavior in mutants—*snail* mutants, which fail to undergo mesoderm invagination, have a lesser degree of cell-shape alignment and a delayed onset of tissue flow.

During epiboly, the first stage of zebrafish embryogenesis, the blastoderm (composed of an epithelial enveloping layer [EVL] covering deep cells) spreads over the massive yolk cell by expanding the EVL and radially contracting via intercalation of deep cells (Bruce, 2016; Morita et al., 2017). The active forces that drive this process are well appreciated; additionally, recent work showed that tuning the mechanical properties of deep cells allows for their passive deformation at the onset of epiboly before radial intercalation has begun (Petridou et al., 2019). Deep cells lose cell-cell junctional integrity as they divide, leading to lower tissue viscosity and fluidization and allowing the expanding EVL to compress the deep-cell layer and drive blastoderm thinning (Figure 1D).

Axis elongation in zebrafish embryos involves extensive collective cell migration and depends upon tissue fluidity (Lawton et al., 2013; Mongera et al., 2018). Cells of the tailbud migrate posteriorly in a coherent fashion until they reach the tip where their movement becomes less coherent, a hallmark of fluidization (Lawton et al., 2013). The observed patterns of cell migration point to a role for graded tissue mechanics in regulating axis elongation. Recently, new biophysical tools have been applied to uncover the mechanical properties of the tailbud and have revealed that axis elongation involves a jamming transition along the anterior-posterior axis (Mongera et al., 2018). A deformable, magnetic oil droplet injected into the tailbud was used to measure local stresses (from passive droplet deformations at rest) and mechanical properties (from active droplet deformation upon application of a magnetic field). These experiments revealed that the fluid-like cells at the tip of the tailbud exhibit lower mechanical integrity than the more solid-like anterior cells that comprise the presomitic mesoderm (PSM). Furthermore, recent work has shown that these tissue mechanical properties are critical components of signal transmission in the tailbud. The cells at the tip of the tailbud form the tailbud organizer and have long been appreciated as an important source of morphogens required for axis elongation. Mechanical information can be communicated between the cells of the tailbud, thus extending the influence of the tail organizer cells beyond the range of morphogen diffusion (Das et al., 2019). The transmission of this mechanical information is likely dependent on the fluidity of the tissue.

The zebrafish tailbud has proven useful for uncovering the physical parameters that regulate fluidity in embryonic tissues. Similar to the deep-cell layer during early epiboly (Petridou et al., 2019), there are greater spaces between cells at the tip of the tailbud that allow for fluid-like behavior (Mongera et al., 2018). Additionally, cell-cell contact lengths are more variable and fluctuate to a greater extent at the tip of the tailbud, and inhibiting myosin activity abrogates this behavior and solidifies the tissue. Finally, cell-cell adhesion supports tissue coherence and solidity in the tailbud, likely by reducing the space between neighboring cells (Lawton et al., 2013; Mongera et al., 2018).

Jamming transitions in embryogenesis are also regulated by cell division and changes in cell phenotype. During gastrulation in chick embryos, cells of the epiblast exhibit dramatic, counter-rotational flows called ''polonaise movements'' that specify the embryonic midline and allow mesendoderm initiation. These rotational movements require cell divisions, without which the epithelial layer is too stable (or solid) for flows to occur (Firmino et al., 2016). Furthermore, recent work combining quantitative live imaging, mechanical modeling, and laser ablations to infer tissue strains in quail embryos showed that the epiblast is surrounded by a supracellular tensile ring that contracts to drive rotational tissue flows and gastrulation (Saadaoui et al., 2020). The onset of neural crest cell migration requires an epithelial-to-mesenchymal transition, which involves a reduction in cell-cell adhesion. In *Xenopus* embryos, internalization of N-cadherin allows neural crest cells to fluidize and thus migrate collectively through narrow spaces (Kuriyama et al., 2014).

Thus far, there are few examples of jamming transitions and roles for tissue solidity and fluidity in organogenesis. In the avian lung, fluidity of the pulmonary mesenchyme helps to distribute the large ECM protein, tenascin, around extending branches (Spurlin et al., 2019). During murine eyelid closure, collective migration of vast epithelial sheets is driven by intercalations of cells at the eyelid front, which may involve localized changes in tissue fluidity (Heller et al., 2014). Jamming transitions have been shown to occur in airway epithelial remodeling in asthma

(Park et al., 2015), raising the possibility that airway epithelial fluidity may also be developmentally regulated as the lung branches and differentiates during embryogenesis.

Physical Constraints and Microenvironmental Mechanics

Developing tissues are subject to a variety of physical constraints, including wrapping by ECM, attachment to a neighboring tissue, and sculpting by surrounding contractile tissues. Physical signals from the tissue microenvironment can elicit cellular behaviors via mechanotransduction (DuFort et al., 2011), and physical constraints can prevent or direct tissue growth or lead to mechanical instabilities and subsequent buckling of tissues (Nelson, 2016).

Changes to basement membrane composition, stiffness, and mechanical integrity provide physical signals that guide tissue morphogenesis (Dzamba and DeSimone, 2018; Walma and Yamada, 2020). The basement membrane around the post-implantation mouse embryo is remodeled to shape the embryo prior to gastrulation and then locally weakened at the posterior pole of the embryo to allow for extension of the primitive streak (Kyprianou et al., 2020). Initially, perforations in the basement membrane around the epiblast allow growth of the embryo along its long axis. As the anterior visceral endoderm migrates from its position at the base of the embryo to the anterior pole, it locally inhibits matrix metalloproteinases, limiting the domain of perforations to the posterior pole. This local reduction in the mechanical integrity of the basement membrane is critical for gastrulation and extension of the primitive streak. Similar basement membrane perforations have been observed at branch tips in the developing salivary gland and are thought to be important for permitting branch growth (Harunaga et al., 2014).

Alterations to tissue mechanical properties can also serve as physical signals that influence the behavior of neighboring tissues. Neural crest cells in the *Xenopus* embryo sense stiffening of the underlying head mesoderm tissue via cell-matrix adhesions (Barriga et al., 2018). This stiffening is required for neural crest development and is itself promoted by morphogenetic movements—convergent extension of the head mesoderm beneath the neural crest cells increases cell density, thus leading to increased stiffness (Barriga et al., 2018). Similar to the example above, stiffening of the underlying endoderm can drive mesenchymal-to-epithelial transition in heart progenitor cells during *Xenopus* embryogenesis (Jackson et al., 2017). Finally, proliferation generates a stiffness gradient in the developing brains of *Xenopus* embryos that is sensed by the retinal ganglion cell axons that migrate along the brain surface (Thompson et al., 2019). Formation of the gradient leads to axon turning, directing them to their destination at the optic tectum.

Growing tissues that are subject to compressive forces from the ECM or from neighboring tissues can fold to relieve the resultant strains. In the developing eye of the chick embryo, the ECM constrains the growing optic vesicle and surface ectoderm, forcing them to invaginate and form the concave optic cup (Oltean et al., 2016). During intestinal morphogenesis in the chick embryo, the small intestine grows faster than the attached dorsal mesentery, resulting in compressive forces along the length of the intestinal tube that lead to looping of the gut into stereotyped patterns (Savin et al., 2011). The wavelength of gut looping depends on differential growth rates between the intestine and the dorsal mesentery, which are regulated by bone morphogenetic protein (BMP) signaling (Nerurkar et al., 2017) and can also be explained by the differences in stiffness between these two connected tissues (Table 1) (Savin et al., 2011). When it is isolated from the surrounding mesenchyme, the murine airway epithelium also undergoes predictable buckling behavior with a wavelength that depends on in-plane compressive forces that are proportional to its growth rate (Table 1) (Varner et al., 2015).

Compressive forces that lead to buckling are often driven by tissue growth and can also be influenced by differences in tissue stiffness or contractility. Constrained growth and mechanical forces imposed by surrounding smooth muscle drive epithelial morphogenesis in the avian intestine (Shyer et al., 2013) and in the murine airway epithelium (Goodwin et al., 2019; Kim et al., 2015). In each of these cases, a uniformly growing epithelial tube achieves complex topologies (folds and zigzags in the intestine, branches and bifurcations in the lung) due to spatiotemporally patterned differentiation of stiff smooth muscle layers from the surrounding mesenchyme.

Forces from the growth of neighboring tissues direct morphogenesis and can also influence differentiation. For example, smooth muscle differentiation in the chick intestine drives epithelial buckling and is itself regulated by strain that results from growth of the epithelial tube (Huycke et al., 2019). Circumferential and longitudinal smooth muscle layers differentiate sequentially during intestinal morphogenesis. Continuous strain from growth of the epithelium aligns the first layer of smooth muscle cells circumferentially and, subsequently, periodic contractions of this first layer longitudinally align the second, outer layer of smooth muscle (Figure 2A).

Static and Dynamic Pressure

Fluid-filled lumens play diverse mechanical and biochemical roles during development, and several experimental techniques have been used to quantify pressure within them (Chan and Hiiragi, 2020). Lumens form when cells release ions and solutes into the extracellular space, generating an osmotic gradient that directs fluid flow. The fluid within the lumen is contained by tight junctions between cells of the tissue surrounding them, and its expansion generates hydrostatic pressure that exerts stress on the cells surrounding the lumen (Table 1). The mechanisms by which cells sense pressure have yet to be fully elucidated and likely vary depending on the context. Pressure may deform the cell cortex, leading to mechanotransduction via actomyosin networks or mechanosensitive ion channels. Osmotic gradients generated by fluid-filled lumens can also affect cytoplasmic fluid content and cell volume, thus changing the pH, salt content, and concentration of proteins within the cytoplasm (Chan and Hiiragi, 2020; Guo et al., 2017).

Recently, several studies have beautifully delineated roles for fluid pressure in lumen coalescence, junctional maturation, and cell allocation during blastocyst development (Chan et al., 2019; Dumortier et al., 2019; Leonavicius et al., 2018; Ryan et al., 2019). Pressure buildup in the blastocyst also helps the embryo to hatch from the zona pellucida, a thick membrane that surrounds the embryo before implantation (Leonavicius et al., 2018). Prior to blastocyst formation, cells of the mouse embryo produce actin-coated vesicles to secrete fluid into the

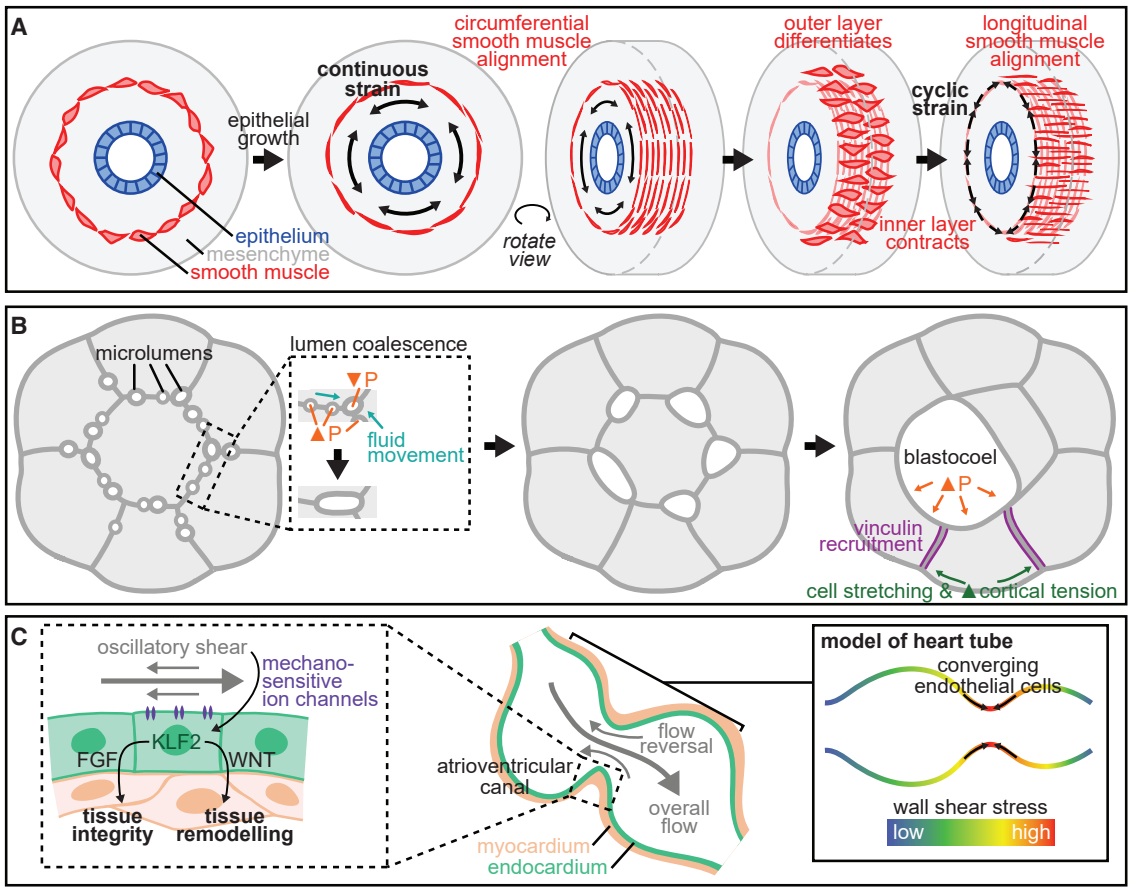

Figure 2. Extrinsic Mechanical Forces Driving Morphogenesis

(A) During chick embryogenesis, growth of the intestinal epithelium generates continuous strain to align the first circumferential layer of smooth muscle cells. Subsequently, periodic contractions of the circumferential smooth muscle layer generate cyclic strain to align the outer longitudinal layer of smooth muscle cells.

(B) Pressurized microlumens form between cells of the early mouse embryo and, as they combine, break embryonic symmetry and establish a single fluid-filled cavity within the blastocyst.

(C) Blood flow drives morphogenesis of the zebrafish heart valve by activating the shear-sensitive transcription factor, KLF2, via mechanosensitive ion channels. Downstream flow-responsive signaling through FGF and WNT is required for maintaining the integrity of the myocardial wall and for driving tissue remodeling. Flow also generates patterns of wall shear stress that predict the direction of endocardial cell convergence toward the AVC.

extracellular space (Ryan et al., 2019). This process produces many microlumens that gradually coalesce to form a single fluid-filled cavity (the blastocoel). The process of lumen coalescence has been likened to hydraulic fracturing: buildup of fluid in microlumens between cells mechanically disrupts local cell-cell contacts (Dumortier et al., 2019). Smaller, more pressurized microlumens discharge their contents into neighboring microlumens and, gradually, all microlumens resolve to form the blastocoel (Figure 2B). As the blastocoel forms and fluid pressure within it increases, trophectoderm cells become stretched and experience higher cortical tension, leading to tight junction maturation and recruitment of the mechanosensory protein, vinculin, to tight junctions (Chan et al., 2019). Accumulation of keratins in the outer cells of the blastocyst may also help the embryo to withstand the increasing pressure in the blastocoel (Lim et al., 2020).

The effects of pressure and tension are inextricably linked in the earliest stages of mouse embryogenesis and cooperate to pattern the embryo. Asymmetries in tension at cell-cell junctions direct lumen coalescence—fluid in lumens at interfaces with higher tension flows into those at interfaces with lower tension, resulting in final blastocoel positioning at the interface between the less contractile trophectoderm cells and the more contractile ICM cells, rather than between ICM cells (Dumortier et al., 2019). Modulating either pressure or cortical tension also affects blastocoel size, which, in turn, shifts the balance between inner cell and trophectoderm cell allocations—smaller cavities favor the ICM at the expense of the trophectoderm, whereas larger cavities position more cells within the trophectoderm and fewer within the ICM (Chan et al., 2019). Finally, sorting of the two cell types that comprise the ICM (the epiblast and primitive endoderm) is coupled to lumen expansion from embryonic day (E) 3.5 to E4 and primitive endoderm specification is sensitive to luminal volume (Ryan et al., 2019). The effects of pressure alone on cell-fate specification within the ICM remain unclear; however, manipulating fluid volume changes the availability of soluble factors that are important for specifying cell fate.

Pressure continues to regulate development at later stages of embryogenesis. During post-implantation mouse development, embryos are subject to external pressures from uterine smooth

muscle contraction. Some of the pressure is absorbed by Reichert's membrane—a specialized basement membrane that encases embryos immediately following implantation—and the fluid-filled space it creates around the developing embryo, which preserves overall embryo morphology (Ueda et al., 2020). During morphogenesis of the chick brain, the neural tube becomes filled with cerebrospinal fluid (CSF) that exerts pressure on the neuroepithelium (Garcia et al., 2019). Combined with morphogen gradients, this pressure drives growth of the left and right cerebral hemispheres; experimentally decreasing CSF pressure prevents hemisphere outgrowth, whereas increasing pressure leads to enlarged hemispheres. During zebrafish inner ear morphogenesis, hydrostatic pressure increases as the epithelial cells of the otic vesicle change shape and secrete fluid into the cavity (Hoijman et al., 2015); the resultant change in pressure in turn regulates the size of the otic vesicle (Mosaliganti et al., 2019). Additionally, patterned actomyosin accumulation along the luminal surface of the otic vesicle allows some cells to resist deformation due to pressure, leading to localized thinning of the epithelium and affecting the shape of the cavity (Hoijman et al., 2015; Mosaliganti et al., 2019).

During development of the mouse lung, static and dynamic pressure drive the formation of complex tissue architecture and influence cell differentiation. Throughout embryogenesis, the lumens of the airways are filled with fluid and the entire organ is encased within the fluid-filled thoracic cavity; the pressure difference between these two compartments generates transmural pressure across the organ. Embryonic lungs isolated at the early stages of branching morphogenesis can be cultured *ex vivo* in a "microfluidic chest cavity" designed to apply transmural pressure (Nelson et al., 2017). Under higher transmural pressure, lung explants undergo more branching and have gene expression profiles that more closely resemble those of lungs that develop within the embryo than lungs cultured under lower transmural pressure. Visualizing branching morphogenesis under pressure in this culture system revealed that synchronized airway smooth muscle contractions every ~12 h preceded near-simultaneous epithelial bifurcations. This observation suggests that smooth muscle contractions could displace luminal fluid toward branch tips, leading to local changes in pressure that induce branching events.

Luminal pressure also drives differentiation of alveolar cell types during the late stages of lung development (Li et al., 2018). Fetal breathing moves luminal fluid toward branch tips, where alveolar progenitors reside. Some of these cells protrude into the mesenchyme, constrict their apical surfaces, and are thus protected from changes in fluid pressure. These cells preferentially give rise to the cuboidal surfactant-producing alveolar type II cells, while their neighbors (which are subjected to the full force of fluid pressure) preferentially give rise to the very thin, elongated, gas-exchanging alveolar type I cells.

Fluid Flow and Shear Forces

Cells that line fluid-filled lumens can be subject not only to hydrostatic or dynamic pressure but also to forces associated with fluid flow. Flow generates shear forces along the walls of the lumen and the magnitude of these forces scales with fluid velocity (Table 1). A wide range of fluid velocities are present throughout the embryo, from weaker flows generated by beating cilia to faster flows generated by the beating heart. Mechanosensitive ion channels are key components of flow sensing, and primary cilia have also been suggested to act as force sensors that bend when exposed to shear stress to initiate downstream signaling cascades (Hyman et al., 2017; Spasic and Jacobs, 2017). However, the role of primary cilia is debated since the entire cell surface could respond to shear forces caused by flow (Ferreira et al., 2019).

Early embryogenesis and establishment of the body plan are orchestrated in part by a small group of cells called the organizer (in amphibians) or the node (in mammals). In particular, left-right patterning is established at the node: 200 to 300 motile cilia at the center of the node generate unidirectional fluid flow, and primary cilia in the cells at the periphery of the node are required to sense this flow (Shinohara et al., 2012; Yoshiba et al., 2012). Flows are highest at the right side of the embryo, increase over the course of development, and reach a velocity of 2–4 μm/s. Whether flow is sensed chemically or mechanically remains a matter of debate (Cartwright et al., 2020). Flow causes spikes in intracellular calcium, supporting the idea that cilia engage in mechanosensing; however, examining this response with higher temporal and spatial resolution revealed that calcium waves do not originate from primary cilia, suggesting that they are not mechanosensing in this context (Delling et al., 2016). However, it is clear that the mechanisms that detect flow are highly sensitive—mutants in which only two cilia are beating (causing a fluid velocity of 1 μm/s that decays toward the periphery of the node) still generate sufficient flow for left-right patterning (Shinohara et al., 2012).

Midway through embryogenesis, once the heart has formed and has started beating, blood flow throughout the developing vascular network becomes a powerful force for tissue morphogenesis (Hyman et al., 2017). Zebrafish embryos with impaired heart development survive much longer than analogous mouse models, making them an excellent model system for studies of cardiovascular development. Flow velocities in the developing zebrafish heart are 3–4 orders of magnitude greater than those at the node (Boselli and Vermot, 2016). Prior to development of the heart valve, blood flow through the heart frequently reverses direction, leading to oscillatory flow and shear stresses on the valve precursor cells of the endocardium (Figure 2C). Oscillatory blood flow is sensed by mechanosensitive ion channels expressed in the endocardium and activates the expression of the shear-responsive gene, Kruppel-like factor 2 (*klf2*); each of these components is required for valve development (Heckel et al., 2015; Vermot et al., 2009).

The mechanisms by which flow and KLF2 drive heart morphogenesis are being uncovered in the zebrafish and in the mouse. KLF2-dependent fibroblast growth factor (FGF) signaling from endocardial cells to their neighboring cardiomyocytes is required to prevent their extrusion and to maintain myocardial wall integrity (Rasouli et al., 2018). In murine heart valve development, shear forces acting through KLF2 activate paracrine signaling from the endocardium to the underlying mesenchymal cells via Wingless-related integration site 9 (WNT9) to drive tissue remodeling (Goddard et al., 2017). Similar morphogenetic events may also occur in the embryonic zebrafish heart, where blood flow and KLF2 are also required for the expression of *Wnt9b* in the endocardium.

Shear stress due to blood flow also predicts patterns of convergent extension in the developing zebrafish heart (Boselli et al., 2017). Labeling endocardial cells with photoconvertible fluorescent markers revealed that they converge toward the atrioventricular canal (AVC) but only in the presence of shear forces caused by blood flow. However, convergence of the endocardial cells toward the AVC cannot be predicted by flow patterns, which are overall unidirectional. A mechanical model of blood flow through a periodically deforming heart tube (which effectively recapitulates flow patterns) predicts that the highest wall shear stresses are experienced by the AVC, suggesting that patterned shear stresses may provide the directional cue for endocardial cell convergence.

Flow also regulates development of organ systems beyond the heart and vasculature. In the developing zebrafish spinal cord, motile cilia drive bidirectional flow of CSF through the central canal that is mechanically sensed by CSF-contacting neurons via the cation channel, polycystic kidney disease 2-like 1 (PKD2L1) (Sternberg et al., 2018). Here, flow velocities are slightly faster than at the node, reaching a maximum of ~5 μm/s, and bidirectionality of the flow is attributed to the presence of motile cilia primarily on the ventral surface of the canal (Thouvenin et al., 2020). CSF within the central canal of the spinal cord is continuous with that bathing the ventricles of the developing brain; separating these compartments by photoablation leads to increased body-axis curvature, suggesting that flow of CSF and/or its constituent particles from the brain to the spinal cord is important for embryonic development. Additionally, PKD2L1 is required for development of a straight spine (Sternberg et al., 2018), suggesting that CSF flow sensing by CSF-contacting neurons broadly regulates morphogenesis of the spinal cord.

CONCLUSIONS AND OUTLOOK

Developmental mechanobiology is a rapidly growing field and new, important questions are being asked. In closing, we wish to highlight two areas that might be of particular interest for future studies of the mechanics of development. First, what powers all of this force generation? There is increasing interest in how regulation of metabolism is coupled to force generation and mechanosensing during development (Perestrelo et al., 2018). Metabolic reprogramming related to the activity of the mechanosensor, Yap, is critical for the first cell-fate specification in early mouse embryos (Chi et al., 2020) and for neural crest migration in avian embryos (Bhattacharya et al., 2020). Classic metabolomic approaches may help to explore this area, but given the inherent complexity of developing tissues, adapting newer techniques in spatial metabolomics may be especially valuable in answering this question.

Second, it is now well appreciated that the nucleus itself is a mechanosensor (Elosegui-Artola et al., 2017; Kirby and Lammerding, 2018). This behavior is evident in cell culture and has been implicated in cancer but has not yet been shown to be relevant to development. The nuclear lamina can mechanically protect the genome and this might play a role in heart development (Cho et al., 2019). Applied strain is resisted by lowering tension in the nuclear envelope and remodeling heterochromatin to prevent DNA damage in cell culture models of epithelial tissues, and there is evidence that this phenomenon may occur within epithelial folds experiencing high levels of tension during murine digit morphogenesis (Nava et al., 2020). However, mouse models of lamin mutations are able to complete embryogenesis and show only partial perinatal lethality, suggesting either that lamins play a minor mechanical role during early development or that their mechanical functions are redundant (Stewart et al., 2007). Molecular tension sensors have successfully been employed to measure forces at the cell cortex in the developing embryo (Lemke et al., 2019; Tao et al., 2019)—similar sensors that permit the measurement of forces at the interface between the cytoskeleton and the nucleus could yield important insights into this question. Additionally, improved imaging capabilities and biophysical measurements that can be applied to intact tissues will undoubtedly elucidate the role of nuclear mechanosensing in development.

ACKNOWLEDGMENTS

Work from the authors' group was supported by awards from the NIH (HD099030, HL120142) and a Faculty Scholars Award from the Howard Hughes Medical Institute. K.G. was supported in part by a postgraduate scholarship-doctoral (PGS-D) from the Natural Sciences and Engineering Research Council of Canada and the Dr. Margaret McWilliams Predoctoral Fellowship from the Canadian Federation of University Women.

REFERENCES

Anlaş, A.A., and Nelson, C.M. (2018). Tissue mechanics regulates form, function, and dysfunction. Curr. Opin. Cell Biol. *54*, 98–105.

Atia, L., Bi, D., Sharma, Y., Mitchel, J.A., Gweon, B., Koehler, S., DeCamp, S.J., Lan, B., Kim, J.H., Hirsch, R., et al. (2018). Geometric constraints during epithelial jamming. Nat. Phys. *14*, 613–620.

Ayad, N.M.E., Kaushik, S., and Weaver, V.M. (2019). Tissue mechanics, an important regulator of development and disease. Philos. Trans. R. Soc. Lond. B *374*, 20180215.

Barriga, E.H., Franze, K., Charras, G., and Mayor, R. (2018). Tissue stiffening coordinates morphogenesis by triggering collective cell migration in vivo. Nature *554*, 523–527.

Beloussov, L.V., Saveliev, S.V., Naumidi, I.I., and Novoselov, V.V. (1994). Mechanical stresses in embryonic tissues: patterns, morphogenetic role, and involvement in regulatory feedback. Int. Rev. Cytol. *150*, 1–34.

Bhattacharya, D., Azambuja, A.P., and Simoes-Costa, M. (2020). Metabolic reprogramming promotes neural crest migration via Yap/tead signaling. Dev. Cell *53*, 199–211.e6.

Bi, D., Lopez, J.H., Schwarz, J.M., and Manning, M.L. (2015). A density-independent rigidity transition in biological tissues. Nat. Phys. *11*, 1074–1079.

Boselli, F., Steed, E., Freund, J.B., and Vermot, J. (2017). Anisotropic shear stress patterns predict the orientation of convergent tissue movements in the embryonic heart. Development *144*, 4322–4327.

Boselli, F., and Vermot, J. (2016). Live imaging and modeling for shear stress quantification in the embryonic zebrafish heart. Methods *94*, 129–134.

Briscoe, J., and Small, S. (2015). Morphogen rules: design principles of gradient-mediated embryo patterning. Development *142*, 3996–4009.

Bruce, A.E. (2016). Zebrafish epiboly: spreading thin over the yolk. Dev. Dyn. *245*, 244–258.

Brunet, T., Larson, B.T., Linden, T.A., Vermeij, M.J.A., McDonald, K., and King, N. (2019). Light-regulated collective contractility in a multicellular choanoflagellate. Science *366*, 326–334.

Cartwright, J.H.E., Piro, O., and Tuval, I. (2020). Chemosensing versus mechanosensing in nodal and Kupffer's vesicle cilia and in other left-right organizer organs. Philos. Trans. R. Soc. Lond. B *375*, 20190566.

Cetera, M., Leybova, L., Joyce, B., and Devenport, D. (2018). Counter-rotational cell flows drive morphological and cell fate asymmetries in mammalian hair follicles. Nat. Cell Biol. *20*, 541–552.

Chan, C.J., Costanzo, M., Ruiz-Herrero, T., Mönke, G., Petrie, R.J., Bergert, M., Diz-Muñoz, A., Mahadevan, L., and Hiiragi, T. (2019). Hydraulic control of mammalian embryo size and cell fate. Nature *571*, 112–116.

Chan, C.J., and Hiiragi, T. (2020). Integration of luminal pressure and signalling in tissue self-organization. Development *147*, dev.181297.

Chi, F., Sharpley, M.S., Nagaraj, R., Roy, S.S., and Banerjee, U. (2020). Glycolysis-independent glucose metabolism distinguishes TE from ICM fate during mammalian embryogenesis. Dev. Cell *53*, 9–26.e4.

Cho, S., Vashisth, M., Abbas, A., Majkut, S., Vogel, K., Xia, Y., Ivanovska, I.L., Irianto, J., Tewari, M., Zhu, K., et al. (2019). Mechanosensing by the lamina protects against nuclear rupture, DNA damage, and cell-cycle arrest. Dev. Cell *49*, 920–935.e5.

Chung, S., Kim, S., and Andrew, D.J. (2017). Uncoupling apical constriction from tissue invagination. eLife *6*, e22235.

Das, D., Jülich, D., Schwendinger-Schreck, J., Guillon, E., Lawton, A.K., Dray, N., Emonet, T., O'Hern, C.S., Shattuck, M.D., and Holley, S.A. (2019). Organization of embryonic morphogenesis via mechanical information. Dev. Cell *49*, 829–839.e5.

Delling, M., Indzhykulian, A.A., Liu, X., Li, Y., Xie, T., Corey, D.P., and Clapham, D.E. (2016). Primary cilia are not calcium-responsive mechanosensors. Nature *531*, 656–660.

DuFort, C.C., Paszek, M.J., and Weaver, V.M. (2011). Balancing forces: architectural control of mechanotransduction. Nat. Rev. Mol. Cell Biol. *12*, 308–319.

Dumortier, J.G., Le Verge-Serandour, M., Tortorelli, A.F., Mielke, A., de Plater, L., Turlier, H., and Maître, J.L. (2019). Hydraulic fracturing and active coarsening position the lumen of the mouse blastocyst. Science *365*, 465–468.

Dzamba, B.J., and DeSimone, D.W. (2018). Extracellular matrix (ECM) and the sculpting of embryonic tissues. Curr. Top. Dev. Biol. *130*, 245–274.

Elosegui-Artola, A., Andreu, I., Beedle, A.E.M., Lezamiz, A., Uroz, M., Kosmalska, A.J., Oria, R., Kechagia, J.Z., Rico-Lastres, P., Le Roux, A.L., et al. (2017). Force triggers YAP nuclear entry by regulating transport across nuclear pores. Cell *171*, 1397–1410.e14.

Fierro-González, J.C., White, M.D., Silva, J.C., and Plachta, N. (2013). Cadherin-dependent filopodia control preimplantation embryo compaction. Nat. Cell Biol. *15*, 1424–1433.

Firmino, J., Rocancourt, D., Saadaoui, M., Moreau, C., and Gros, J. (2016). Cell division drives epithelial cell rearrangements during gastrulation in chick. Dev. Cell *36*, 249–261.

Freeman, M., and Gurdon, J.B. (2002). Regulatory principles of developmental signaling. Annu. Rev. Cell Dev. Biol. *18*, 515–539.

Garcia, K.E., Stewart, W.G., Espinosa, M.G., Gleghorn, J.P., and Taber, L.A. (2019). Molecular and mechanical signals determine morphogenesis of the cerebral hemispheres in the chicken embryo. Development *146*, dev174318.

Goddard, L.M., Duchemin, A.L., Ramalingan, H., Wu, B., Chen, M., Bamezai, S., Yang, J., Li, L., Morley, M.P., Wang, T., et al. (2017). Hemodynamic forces sculpt developing heart valves through a KLF2-WNT9B paracrine signaling axis. Dev. Cell *43*, 274–289.e5.

Goodwin, K., Mao, S., Guyomar, T., Miller, E., Radisky, D.C., Košmrlj, A., and Nelson, C.M. (2019). Smooth muscle differentiation shapes domain branches during mouse lung development. Development *146*, dev181172.

Guo, M., Pegoraro, A.F., Mao, A., Zhou, E.H., Arany, P.R., Han, Y., Burnette, D.T., Jensen, M.H., Kasza, K.E., Moore, J.R., et al. (2017). Cell volume change through water efflux impacts cell stiffness and stem cell fate. Proc. Natl. Acad. Sci. USA *114*, E8618–E8627.

Haeger, A., Krause, M., Wolf, K., and Friedl, P. (2014). Cell jamming: collective invasion of mesenchymal tumor cells imposed by tissue confinement. Biochim. Biophys. Acta *1840*, 2386–2395.

Hampoelz, B., and Lecuit, T. (2011). Nuclear mechanics in differentiation and development. Curr. Opin. Cell Biol. *23*, 668–675.

Harunaga, J.S., Doyle, A.D., and Yamada, K.M. (2014). Local and global dynamics of the basement membrane during branching morphogenesis require protease activity and actomyosin contractility. Dev. Biol. *394*, 197–205.

Heckel, E., Boselli, F., Roth, S., Krudewig, A., Belting, H.G., Charvin, G., and Vermot, J. (2015). Oscillatory flow modulates mechanosensitive klf2a expression through trpv4 and trpp2 during heart valve development. Curr. Biol. *25*, 1354–1361.

Heisenberg, C.P., and Bellaïche, Y. (2013). Forces in tissue morphogenesis and patterning. Cell *153*, 948–962.

Heller, E., Kumar, K.V., Grill, S.W., and Fuchs, E. (2014). Forces generated by cell intercalation tow epidermal sheets in mammalian tissue morphogenesis. Dev. Cell *28*, 617–632.

Hoffman, B.D., Grashoff, C., and Schwartz, M.A. (2011). Dynamic molecular processes mediate cellular mechanotransduction. Nature *475*, 316–323.

Hoijman, E., Rubbini, D., Colombelli, J., and Alsina, B. (2015). Mitotic cell rounding and epithelial thinning regulate lumen growth and shape. Nat. Commun. *6*, 7355.

Huycke, T.R., Miller, B.M., Gill, H.K., Nerurkar, N.L., Sprinzak, D., Mahadevan, L., and Tabin, C.J. (2019). Genetic and mechanical regulation of intestinal smooth muscle development. Cell *179*, 90–105.e21.

Hyman, A.J., Tumova, S., and Beech, D.J. (2017). Piezo1 channels in vascular development and the sensing of shear stress. Curr. Top. Membr. *79*, 37–57.

Jackson, T.R., Kim, H.Y., Balakrishnan, U.L., Stuckenholz, C., and Davidson, L.A. (2017). Spatiotemporally controlled mechanical cues drive progenitor mesenchymal-to-epithelial transition enabling proper heart formation and function. Curr. Biol. *27*, 1326–1335.

Keller, R., Davidson, L.A., and Shook, D.R. (2003). How we are shaped: the biomechanics of gastrulation. Differentiation *71*, 171–205.

Kicheva, A., and Briscoe, J. (2015). Developmental pattern formation in phases. Trends Cell Biol. *25*, 579–591.

Kim, H.Y., Pang, M.F., Varner, V.D., Kojima, L., Miller, E., Radisky, D.C., and Nelson, C.M. (2015). Localized smooth muscle differentiation is essential for epithelial bifurcation during branching morphogenesis of the mammalian lung. Dev. Cell *34*, 719–726.

Kim, H.Y., Varner, V.D., and Nelson, C.M. (2013). Apical constriction initiates new bud formation during monopodial branching of the embryonic chicken lung. Development *140*, 3146–3155.

Kirby, T.J., and Lammerding, J. (2018). Emerging views of the nucleus as a cellular mechanosensor. Nat. Cell Biol. *20*, 373–381.

Kumar, A., Placone, J.K., and Engler, A.J. (2017). Understanding the extracellular forces that determine cell fate and maintenance. Development *144*, 4261–4270.

Kuriyama, S., Theveneau, E., Benedetto, A., Parsons, M., Tanaka, M., Charras, G., Kabla, A., and Mayor, R. (2014). In vivo collective cell migration requires an LPAR2-dependent increase in tissue fluidity. J. Cell Biol. *206*, 113–127.

Kyprianou, C., Christodoulou, N., Hamilton, R.S., Nahaboo, W., Boomgaard, D.S., Amadei, G., Migeotte, I., and Zernicka-Goetz, M. (2020). Basement membrane remodelling regulates mouse embryogenesis. Nature *582*, 253–258.

Lawton, A.K., Nandi, A., Stulberg, M.J., Dray, N., Sneddon, M.W., Pontius, W., Emonet, T., and Holley, S.A. (2013). Regulated tissue fluidity steers zebrafish body elongation. Development *140*, 573–582.

Lecuit, T., and Lenne, P.F. (2007). Cell surface mechanics and the control of cell shape, tissue patterns and morphogenesis. Nat. Rev. Mol. Cell Biol. *8*, 633–644.

Lemke, S.B., Weidemann, T., Cost, A.L., Grashoff, C., and Schnorrer, F. (2019). A small proportion of Talin molecules transmit forces at developing muscle attachments in vivo. PLoS Biol. *17*, e3000057.

Leonavicius, K., Royer, C., Preece, C., Davies, B., Biggins, J.S., and Srinivas, S. (2018). Mechanics of mouse blastocyst hatching revealed by a hydrogel-based microdeformation assay. Proc. Natl. Acad. Sci. USA *115*, 10375–10380.

Li, J., Wang, Z., Chu, Q., Jiang, K., Li, J., and Tang, N. (2018). The strength of mechanical forces determines the differentiation of alveolar epithelial cells. Dev. Cell *44*, 297–312.e5.

Lim, H.Y.G., Alvarez, Y.D., Gasnier, M., Wang, Y., Tetlak, P., Bissiere, S., Wang, H., Biro, M., and Plachta, N. (2020). Keratins are asymmetrically inherited fate determinants in the mammalian embryo. Nature *585*, 404–409.

Maître, J.L., Niwayama, R., Turlier, H., Nédélec, F., and Hiiragi, T. (2015). Pulsatile cell-autonomous contractility drives compaction in the mouse embryo. Nat. Cell Biol. *17*, 849–855.

Maître, J.L., Turlier, H., Illukkumbura, R., Eismann, B., Niwayama, R., Nédélec, F., and Hiiragi, T. (2016). Asymmetric division of contractile domains couples cell positioning and fate specification. Nature *536*, 344–348.

Mammoto, T., and Ingber, D.E. (2010). Mechanical control of tissue and organ development. Development *137*, 1407–1420.

Manning, L.A., Weideman, A.M., Peercy, B.E., and Starz-Gaiano, M. (2015). Tissue landscape alters adjacent cell fates during Drosophila egg development. Nat. Commun. *6*, 7356.

Martin, A.C., Kaschube, M., and Wieschaus, E.F. (2009). Pulsed contractions of an actin-myosin network drive apical constriction. Nature *457*, 495–499.

Mongera, A., Rowghanian, P., Gustafson, H.J., Shelton, E., Kealhofer, D.A., Carn, E.K., Serwane, F., Lucio, A.A., Giammona, J., and Campàs, O. (2018). A fluid-to-solid jamming transition underlies vertebrate body axis elongation. Nature *561*, 401–405.

Morita, H., Grigolon, S., Bock, M., Krens, S.F., Salbreux, G., and Heisenberg, C.P. (2017). The physical basis of coordinated tissue spreading in zebrafish gastrulation. Dev. Cell *40*, 354–366.e4.

Mosaliganti, K.R., Swinburne, I.A., Chan, C.U., Obholzer, N.D., Green, A.A., Tanksale, S., Mahadevan, L., and Megason, S.G. (2019). Size control of the inner ear via hydraulic feedback. eLife *8*, e39596.

Nava, M.M., Miroshnikova, Y.A., Biggs, L.C., Whitefield, D.B., Metge, F., Boucas, J., Vihinen, H., Jokitalo, E., Li, X., García Arcos, J.M., et al. (2020). Heterochromatin-driven nuclear softening protects the genome against mechanical stress-induced damage. Cell *181*, 800–817.e22.

Nelson, C.M. (2016). On buckling morphogenesis. J. Biomech. Eng. *138*, 021005.

Nelson, C.M., Gleghorn, J.P., Pang, M.F., Jaslove, J.M., Goodwin, K., Varner, V.D., Miller, E., Radisky, D.C., and Stone, H.A. (2017). Microfluidic chest cavities reveal that transmural pressure controls the rate of lung development. Development *144*, 4328–4335.

Nerurkar, N.L., Lee, C., Mahadevan, L., and Tabin, C.J. (2019). Molecular control of macroscopic forces drives formation of the vertebrate hindgut. Nature *565*, 480–484.

Nerurkar, N.L., Mahadevan, L., and Tabin, C.J. (2017). BMP signaling controls buckling forces to modulate looping morphogenesis of the gut. Proc. Natl. Acad. Sci. USA *114*, 2277–2282.

Nikolopoulou, E., Galea, G.L., Rolo, A., Greene, N.D., and Copp, A.J. (2017). Neural tube closure: cellular, molecular and biomechanical mechanisms. Development *144*, 552–566.

Oltean, A., Huang, J., Beebe, D.C., and Taber, L.A. (2016). Tissue growth constrained by extracellular matrix drives invagination during optic cup morphogenesis. Biomech. Model. Mechanobiol. *15*, 1405–1421.

Park, J.A., Kim, J.H., Bi, D., Mitchel, J.A., Qazvini, N.T., Tantisira, K., Park, C.Y., McGill, M., Kim, S.H., Gweon, B., et al. (2015). Unjamming and cell shape in the asthmatic airway epithelium. Nat. Mater. *14*, 1040–1048.

Perestrelo, T., Correia, M., Ramalho-Santos, J., and Wirtz, D. (2018). Metabolic and mechanical cues regulating pluripotent stem cell fate. Trends Cell Biol. *28*, 1014–1029.

Petridou, N.I., Grigolon, S., Salbreux, G., Hannezo, E., and Heisenberg, C.P. (2019). Fluidization-mediated tissue spreading by mitotic cell rounding and non-canonical Wnt signalling. Nat. Cell Biol. *21*, 169–178.

Ferreira, R.R., Fukui, H., Chow, R., Vilfan, A., and Vermot, J. (2019). The cilium as a force sensor-myth versus reality. J. Cell Sci. *132*, jcs213496.

Rasouli, S.J., El-Brolosy, M., Tsedeke, A.T., Bensimon-Brito, A., Ghanbari, P., Maischein, H.M., Kuenne, C., and Stainier, D.Y. (2018). The flow responsive transcription factor Klf2 is required for myocardial wall integrity by modulating Fgf signaling. eLife *7*, e38889.

Ryan, A.Q., Chan, C.J., Graner, F., and Hiiragi, T. (2019). Lumen expansion facilitates epiblast-primitive endoderm fate specification during mouse blastocyst formation. Dev. Cell *51*, 684–697.e4.

Saadaoui, M., Rocancourt, D., Roussel, J., Corson, F., and Gros, J. (2020). A tensile ring drives tissue flows to shape the gastrulating amniote embryo. Science *367*, 453–458.

Samarage, C.R., White, M.D., Álvarez, Y.D., Fierro-González, J.C., Henon, Y., Jesudason, E.C., Bissiere, S., Fouras, A., and Plachta, N. (2015). Cortical tension allocates the first inner cells of the mammalian embryo. Dev. Cell *34*, 435–447.

Savin, T., Kurpios, N.A., Shyer, A.E., Florescu, P., Liang, H., Mahadevan, L., and Tabin, C.J. (2011). On the growth and form of the gut. Nature *476*, 57–62.

Schötz, E.M., Lanio, M., Talbot, J.A., and Manning, M.L. (2013). Glassy dynamics in three-dimensional embryonic tissues. J. R. Soc. Interface *10*, 20130726.

Shinohara, K., Kawasumi, A., Takamatsu, A., Yoshiba, S., Botilde, Y., Motoyama, N., Reith, W., Durand, B., Shiratori, H., and Hamada, H. (2012). Two rotating cilia in the node cavity are sufficient to break left-right symmetry in the mouse embryo. Nat. Commun. *3*, 622.

Shyer, A.E., Huycke, T.R., Lee, C., Mahadevan, L., and Tabin, C.J. (2015). Bending gradients: how the intestinal stem cell gets its home. Cell *161*, 569–580.

Shyer, A.E., Rodrigues, A.R., Schroeder, G.G., Kassianidou, E., Kumar, S., and Harland, R.M. (2017). Emergent cellular self-organization and mechanosensation initiate follicle pattern in the avian skin. Science *357*, 811–815.

Shyer, A.E., Tallinen, T., Nerurkar, N.L., Wei, Z., Gil, E.S., Kaplan, D.L., Tabin, C.J., and Mahadevan, L. (2013). Villification: how the gut gets its villi. Science *342*, 212–218.

Soleas, J.P., D'Arcangelo, E., Huang, L., Karoubi, G., Nostro, M.C., McGuigan, A.P., and Waddell, T.K. (2020). Assembly of lung progenitors into developmentally-inspired geometry drives differentiation via cellular tension. Biomaterials *254*, 120128.

Spasic, M., and Jacobs, C.R. (2017). Primary cilia: cell and molecular mechanosensors directing whole tissue function. Semin. Cell Dev. Biol. *71*, 42–52.

Spurlin, J.W., Siedlik, M.J., Nerger, B.A., Pang, M.F., Jayaraman, S., Zhang, R., and Nelson, C.M. (2019). Mesenchymal proteases and tissue fluidity remodel the extracellular matrix during airway epithelial branching in the embryonic avian lung. Development *146*, dev175257.

Sternberg, J.R., Prendergast, A.E., Brosse, L., Cantaut-Belarif, Y., Thouvenin, O., Orts-Del'Immagine, A., Castillo, L., Djenoune, L., Kurisu, S., McDearmid, J.R., et al. (2018). Pkd2l1 is required for mechanoception in cerebrospinal fluid-contacting neurons and maintenance of spine curvature. Nat. Commun. *9*, 3804.

Stewart, C.L., Kozlov, S., Fong, L.G., and Young, S.G. (2007). Mouse models of the laminopathies. Exp. Cell Res. *313*, 2144–2156.

Stooke-Vaughan, G.A., and Campàs, O. (2018). Physical control of tissue morphogenesis across scales. Curr. Opin. Genet. Dev. *51*, 111–119.

Sumigray, K.D., Terwilliger, M., and Lechler, T. (2018). Morphogenesis and compartmentalization of the intestinal crypt. Dev. Cell *45*, 183–197.e5.

Tao, H., Zhu, M., Lau, K., Whitley, O.K.W., Samani, M., Xiao, X., Chen, X.X., Hahn, N.A., Liu, W., Valencia, M., et al. (2019). Oscillatory cortical forces promote three dimensional cell intercalations that shape the murine mandibular arch. Nat. Commun. *10*, 1703.

Thompson, A.J., Pillai, E.K., Dimov, I.B., Foster, S.K., Holt, C.E., and Franze, K. (2019). Rapid changes in tissue mechanics regulate cell behaviour in the developing embryonic brain. eLife *8*, e39356.

Thouvenin, O., Keiser, L., Cantaut-Belarif, Y., Carbo-Tano, M., Verweij, F., Jurisch-Yaksi, N., Bardet, P.L., van Niel, G., Gallaire, F., and Wyart, C. (2020). Origin and role of the cerebrospinal fluid bidirectional flow in the central canal. eLife *9*, e47699.

Ueda, Y., Kimura-Yoshida, C., Mochida, K., Tsume, M., Kameo, Y., Adachi, T., Lefebvre, O., Hiramatsu, R., and Matsuo, I. (2020). Intrauterine pressures adjusted by Reichert's membrane are crucial for early mouse morphogenesis. Cell Rep. *31*, 107637.

Varner, V.D., Gleghorn, J.P., Miller, E., Radisky, D.C., and Nelson, C.M. (2015). Mechanically patterning the embryonic airway epithelium. Proc. Natl. Acad. Sci. USA *112*, 9230–9235.

Vermot, J., Forouhar, A.S., Liebling, M., Wu, D., Plummer, D., Gharib, M., and Fraser, S.E. (2009). Reversing blood flows act through klf2a to ensure normal valvulogenesis in the developing heart. PLoS Biol. *7*, e1000246.

Vining, K.H., and Mooney, D.J. (2017). Mechanical forces direct stem cell behaviour in development and regeneration. Nat. Rev. Mol. Cell Biol. *18*, 728–742.

Walma, D.A.C., and Yamada, K.M. (2020). The extracellular matrix in development. Development *147*, dev175596.

Wang, X., Merkel, M., Sutter, L.B., Erdemci-Tandogan, G., Manning, M.L., and Kasza, K.E. (2020). Anisotropy links cell shapes to tissue flow during convergent extension. Proc. Natl. Acad. Sci. USA *117*, 13541–13551.

Wolpert, L. (1971). Positional information and pattern formation. Curr. Top. Dev. Biol. *6*, 183–224.

Yoshiba, S., Shiratori, H., Kuo, I.Y., Kawasumi, A., Shinohara, K., Nonaka, S., Asai, Y., Sasaki, G., Belo, J.A., Sasaki, H., et al. (2012). Cilia at the node of mouse embryos sense fluid flow for left-right determination via Pkd2. Science *338*, 226–231.

Zenker, J., White, M.D., Gasnier, M., Alvarez, Y.D., Lim, H.Y.G., Bissiere, S., Biro, M., and Plachta, N. (2018). Expanding actin rings zipper the mouse embryo for blastocyst formation. Cell *173*, 776–791.e17.